

Transient enhanced diffusion of oxygen in Fe mediated by large electronic excitationD. K. Avasthi,¹ W. Assmann,² A. Tripathi,¹ S. K. Srivastava,¹ S. Ghosh,¹ F. Grüner,² and M. Toulemonde³¹*Nuclear Science Centre, Post Box 10502, New Delhi-110067, India*²*Ludwig Maximilians Universität, Garching 85748, Germany*³*CIRIL, CAEN, France*

(Received 2 May 2003; published 27 October 2003)

Contrary to the electronic excitation induced phenomena of desorption and sputtering, we observed incorporation of oxygen in a thin Fe film during its irradiation with swift heavy ions. It is observed that the adsorbed oxygen diffuses in to the Fe film. The incorporation of oxygen and its diffusion in the bulk of the film is a manifestation of extremely large electronic energy deposition by the incident ions. It is shown that the experimentally observed high diffusivity of oxygen in Fe during irradiation is due to the existence of transient melt phase of Fe.

DOI: 10.1103/PhysRevB.68.153106

PACS number(s): 61.80.Jh, 61.82.Bg, 66.30.-h

The swift heavy ions (SHI's) are of interest for materials modification¹⁻⁵ due to their capability of imparting large electronic excitation to the atoms of the material, and materials characterization by elastic recoil detection analysis (ERDA).⁶⁻⁸ The energy loss in this energy regime (>1 MeV/amu) is dominantly via inelastic collisions (electronic stopping) of ions with the atoms, leading to excitation or ionization of atoms, as opposed to the energy loss by dominant elastic collisions (nuclear stopping) in the low energy regime (a few keV/amu). Ejection of atomic, molecular or cluster species from materials under SHI irradiation, a phenomenon also known as electronic sputtering, has attracted a large number of researchers.⁹⁻¹⁹

In the present work, the diffusion of oxygen adsorbed on the surface of an iron thin film into the film is observed and investigated. The incorporation of oxygen during ion irradiation and its diffusion inside the Fe film is just opposite to the ion beam induced desorption or sputtering of atoms, clusters and other species observed so far.⁹⁻¹⁹ High diffusivity of oxygen under the influence of large electronic excitation is explained on the basis of thermal spike formalism.²⁰⁻²² It is proposed that the incident ion produces a molten zone of nanometric size along its path in a typical picosecond time (as predicted by the thermal spike model developed for electronic stopping power regime) and the diffusion of oxygen from surface to inside the film takes place during the melt phase.

Diffusion of oxygen across CuO/float glass interface under influence of electronic excitation has previously been observed and explained as a diffusion process in transient melt phase.²³ Ion beam mixing in oxide/oxide system has also been explained on similar basis.²⁴ In these works, the radius and duration of transient molten zone were taken from the existing thermal spike calculations for insulators. In the present work, the diffusion of adsorbed oxygen in Fe, too, is explained on similar basis, but the importance of the present work is that the concept of diffusion in transient melt phase is quantitatively extended to a metal case. Apart from this, (i) theoretical calculations of thermal spike, required for this purpose, are performed and are a part of the present work and (ii) the adsorption of oxygen and its subsequent diffusion

in the film is rather new observation, contrary to the phenomena of desorption and sputtering induced by energetic ions.

There have been several²⁵⁻²⁷ in-situ measurements of electrical resistivity during ion irradiation in Fe to show the sensitive effect of electronic excitation beyond a threshold of dE/dx on the electronic charge transport. We show the transport of oxygen atoms in Fe film due to similar effects by on-line ERDA measurement.

Three separate experiments were performed to ensure the reproducibility of the observed phenomenon. Au ions of 210, 243 MeV and I ions of 210 MeV (from the Munich MP Tandem accelerator) were incident at 10° relative to the surface (80° to the surface normal) of an about 50 nm thin Fe film evaporated on Si. The electronic energy loss (S_e) values²⁸ for these ions in Fe are around 46, 47, and 36 keV/nm, respectively. The corresponding values²⁸ for nuclear energy loss (S_n) are two orders of magnitude smaller. The vacuum in the chamber was 8×10^{-7} mbar. The ion current was about 0.2 particle nA (1 particle nA = 6.2×10^9 ions s^{-1}) and the beam size was about 0.75 mm² with the use of a collimator. The recoils were detected by a position sensitive gaseous ionization detector (having a solid angle of 5.7 msr) at a scattering angle of 37° . All the signals ($\Delta E, E$, position signals and the integrated current from the sample holder) were stored event by event. The integrated current counts on the target were calibrated with a secondary electron suppressed Faraday cup. The total ion fluence on the samples was about 2 to 4×10^{14} ions/cm². Details of the experimental setup and the analysis of recorded on-line ERD data are available in Refs. 7,8, and references therein. The ion fluence measurement has an uncertainty up to 20% but the relative error between different measurements is less than 1%.

The recorded data in each experiment were divided in ten to twelve equal bins of the ion fluence. The total count under the peak corresponding to a bin is such that the statistical error is $\sim 2-3\%$. The two dimensional $\Delta E-E$ spectra corresponding to oxygen recoils were projected onto the E axis to generate one-dimensional recoil energy spectra of oxygen. Figure 1 shows two such spectra generated for two different ion fluences, corresponding to the first and last bins, of 210 MeV Au. Data only for these two bins have been presented

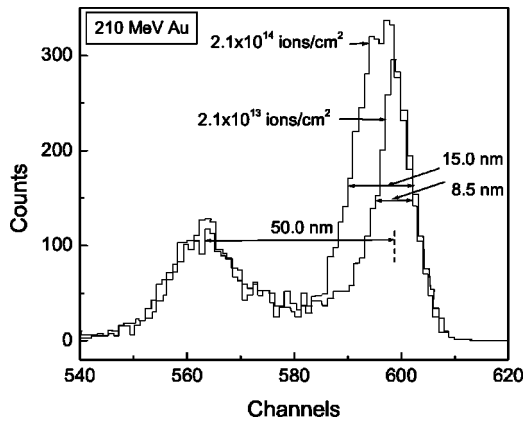


FIG. 1. Recoil spectra of oxygen for 210 MeV Au ions incident on thin Fe film deposited on Si at two fluences corresponding to the first and last bin for the same incident ion charge. It had a narrow peak in the beginning at a fluence of 2.1×10^{13} ions/cm², which broadened due to absorption and diffusion of oxygen at a fluence of 2.1×10^{14} ions/cm².

in the figure for the sake of better clarity. The conversion of recoil energy to depth is obtained by using (i) the kinematics equations and (ii) the energy loss values of the incident ions and the oxygen recoils as calculated from TRIM.²⁸ It is evident from the figure that the content of oxygen inside iron, and the full width at half maximum (FWHM) of the oxygen peak, increase with the ion fluence. This increase in FWHM indicates that the oxygen keeps on diffusing in the Fe film with fluence. The carbon recoil spectra do not change significantly from the beginning to the end, suggesting that there has been no hydrocarbon deposition on the beam spot during ion irradiation. The measurements were repeated with another sample of Fe/Si, which also show the similar trend of increase in oxygen content into the iron film with ion fluence. Similar behavior is observed for the cases of 243 MeV Au and 210 MeV I irradiations.

We will now address two basic issues. (i) What is the origin of the oxygen being incorporated into the Fe film? (ii) What is the possible mechanism of unusually high diffusivity of oxygen in iron during irradiation?

The origin of oxygen is attributed to the presence of several monolayers of H₂O molecules on the sample surface in high vacuum conditions. At the pressure (8×10^{-7} mbar) of the experimental chamber, there are $\sim 3 \times 10^{14}$ H₂O molecules, which are the dominant outgassing species from an Al chamber, striking the sample surface per centimeter square per second. The arrival rate of ions, on the other hand, is only about 3×10^{10} ions cm⁻² s⁻¹, four orders of magnitude smaller than the H₂O impingement rate, for the ion current of 0.2 pA. It can, thus, be safely assumed that each incoming ion encounters a large number of water molecules on the sample surface. This encounter leads to breakage of water molecules due to large electronic excitation. Information on the behavior of water under heavy ion irradiation is scarce. However, dissociation cross section of water in its gas phase²⁹ being $\sim 10^{-14}$ cm² under irradiation with Xe beam at 6 MeV/u, it is reasonable to believe this cross section to be much larger when irradiating the water in its liquid

phase, mainly due to the ionization of water molecules by the δ electrons. Consequently, one can assume that there is a sufficiently large number of dissociated oxygen available at the sample surface to be incorporated into the film. From the oxygen concentration profile, it is clear that the oxygen peak gets broadened during the irradiation, indicating the diffusion of oxygen inside the bulk due to irradiation.

We will now discuss the mechanism of diffusion of oxygen in Fe thin film, subsequent to passage of swift heavy ion. The measurements of such diffusion using the inputs from thermal spike model will be a severe test of the model based on atomic transport measurement. The first such test²⁰⁻²² of the model has been based on the explanation of the annealing and creation of defects beyond certain S_e , observed in the *in situ* resistivity measurements (electronic transport). Using an electron-phonon coupling deduced from electrical resistivity measurements, Wang *et al.*²⁰ have shown that the threshold of damage creation in 10 MeV/u ion irradiated iron, is around 30 keV/nm, if the observed defect results from the quench of a melt phase. With the same set of parameters, the annealing of defects created by nuclear energy loss has been explained,²² taking into account of their activation energy and corroborating that the defect creation by electronic excitation results from the appearance of a melt phase. Since the S_e values in the present experiment are larger than the threshold for damage creation, latent tracks do exist in Fe film. We assume that the diffusion of oxygen in Fe takes place during the transient melt phase and that the diffusion process is not influenced by the ionic nature of diffusing oxygen. The reason for the latter is that the ionic state diffusion is governed by the existence of an electric field gradient, the generation of which in metallic Fe layer is impossible. Thus, from the fluence dependence of FWHM of the oxygen peaks, it is possible to determine the diffusion coefficient, and it should correspond to the diffusivity of oxygen impurity in molten Fe. Thermal spike model²⁰⁻²² calculations are performed for the present ion beam parameters and target combinations, to determine the duration and radius of the melt phase.

Let us first go through the sequence of ion transit through material, the production of recoils, and the ion induced modification. The typical transit time of such ions across an atomic distance is $\sim 10^{-17}$ s. Therefore, the recoils are generated in a time scale of 10^{-17} s with a probability governed by Rutherford recoil cross section. Each incident ion loses its energy, dominantly by electronic excitation, during its transit across the material. Temperature of electronic system rises in a typical time span of 10^{-15} s. It is followed by transfer of energy from electrons to the target via the electron phonon coupling ($\sim 1.44 \times 10^{12}$ W cm⁻³ K⁻¹ for iron), inducing the local temperature rise in a very narrow zone (up to a few thousand K), limited to the short duration of transient temperature spike. The rise and decay of the lattice temperature is governed by two coupled differential equations.²⁰⁻²² Simulations of the evolution of the lattice temperature with time for the three ions have been made and one such set for one of the ions, viz., 210 MeV Au, in Fe, is shown in Fig. 2. For the temperatures above the melting point the lattice melts, followed by fast quenching. The melting of lattice facilitates

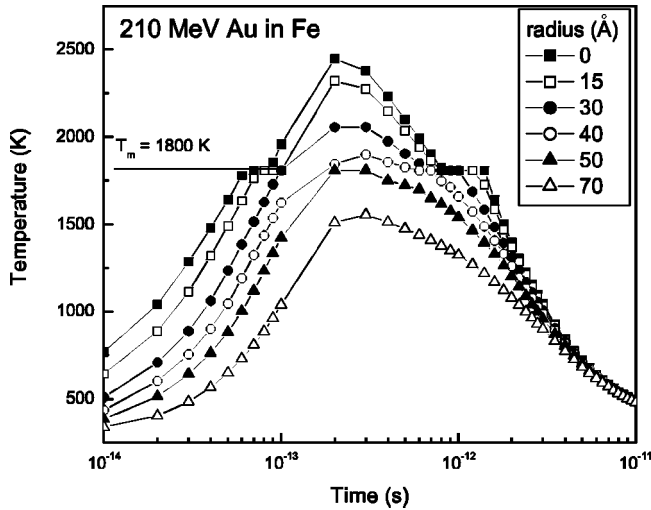


FIG. 2. Plot of lattice temperature rise with time obtained with thermal spike calculation for 210 MeV Au ions in Fe.

atomic motion through this zone and an enhanced diffusion takes place dominantly in each cylindrical melt zone, as the diffusivity in molten state is several orders of magnitude higher than that in the corresponding solid.

Now we focus on the modifications induced by ions and their observation through ERDA. Each ion produces an effective zone of damage within which the modification (diffusion of oxygen in Fe film) is produced. As we are looking for the oxygen diffusion during the on-line ERDA experiment, the first ion generates an oxygen recoil in a time scale (10^{-17} s) much shorter than the thermal spike time (10^{-13} – 10^{-12} s). Consequently the recoil from this ion does not provide any information on the modification produced in iron. However, the recoils generated by subsequent ions hitting a zone which has been already irradiated, will provide the information on the modifications in the lattice. So, after certain fluence ϕ_c , corresponding approximately to d^{-2} , the whole sample surface will be completely irradiated for the first time. Here d is the track diameter. The subsequent ions will then provide information about $(n-1)$ times modifications in the lattice, where n is the number of overlaps of ion fluence (ϕ_c) and is given by ϕ_f/ϕ_c , where ϕ_f is the total fluence. Therefore, the time t for enhanced diffusion will be $(n-1)t_s$, where t_s is the duration of transient melt phase.

The diffusion during transient thermal spike follows the equation

$$D = (\Omega_t^2 - \Omega_0^2) / 2t, \quad (1)$$

where Ω_t is the spatial width of oxygen in Fe after diffusion time t and Ω_0 is the initial spatial width of oxygen in Fe. For the fluence ϕ_i , corresponding to the first bin data, diffusion time $t_i = (d^2\phi_i - 1)t_s$. Similarly, for the fluence ϕ_f , corresponding to the last bin data, diffusion time $t_f = (d^2\phi_f - 1)t_s$. Therefore diffusion time for the observed changes in depth distribution of oxygen in Fe from fluence ϕ_i to fluence ϕ_f can be expressed as

$$t = d^2(\phi_f - \phi_i)t_s. \quad (2)$$

Thermal spike model calculations predict a track diameter of about 8 nm and melt duration of 1.1 ps for 210 MeV Au

ions incident on Fe film. For this track diameter, the Fe film will be completely irradiated for the first time at a fluence (ϕ_c) of $\sim 1.6 \times 10^{12}$ ions/cm². One can then say that at this fluence the oxygen diffusion in Fe took place for a duration of about 1.1 ps. The FWHM of oxygen peaks are 8.5 nm and 15.0 nm corresponding to the fluence (ϕ_i) of 2.1×10^{13} ions/cm² (for the first bin data) and fluence (ϕ_f) 2.1×10^{14} ions/cm² (for the tenth bin data), respectively. Therefore, $\Delta\phi = 19.9 \times 10^{13}$ ions/cm² and thus diffusion coefficient D using Eqs. (1) and (2) is 5.6×10^{-7} m² s⁻¹.

Similarly, the diffusivity of oxygen in Fe is determined for the experiments with 243 MeV of Au ion and 210 MeV of I ion, where the FWHM of oxygen peak increased from 18.6 nm to 30.3 nm for fluence from 2.1×10^{13} ions/cm² to 4.6×10^{14} ions/cm² and from 7.5 nm to 13.5 nm for fluence from 3.8×10^{13} ions/cm² to 3.8×10^{14} ions/cm², respectively. The corresponding average diameters of the melt phase are 10 and 4.5 nm with the average durations of melt phase as 1.32 and 0.75 ps, respectively, as extracted from the thermal spike calculations. The values of diffusivity so obtained are 5.0×10^{-7} and 1.2×10^{-6} m² s⁻¹, respectively for the two cases. Such a high diffusivity of oxygen in Fe is possible only in the molten phase since the value^{30–32} in solid Fe even at temperatures close to the melting temperature (1811 K) is about 10^{-10} m² s⁻¹. The experimental error is up to 40%, taking into account of the error in fluence measurement and the uncertainty in energy loss data used for the conversion of recoil energy to depth scale. The present measured value of diffusivity of oxygen in molten Fe is in fair agreement with other recent ion beam measurements related to diffusion in transient melt phase.^{23,24} If, on the other hand, one assumes that the diffusion has taken place in the solid state of Fe during irradiation (for example, ~ 1150 s for the case of 210 MeV Au irradiation), the diffusivity becomes $\sim 6.4 \times 10^{-20}$ m² s⁻¹. It should be noticed here that the sample remains effectively at room temperature in this duration. A reported solid state diffusivity of oxygen in Fe,³² scaled down to room temperature, is $\sim 3.4 \times 10^{-23}$ m² s⁻¹, three orders of magnitude less than the presently estimated solid state diffusivity. This contradicts the assumption that the diffusion has taken place in the solid state. Moreover, it has been shown for the oxidation of Fe that at room temperature the oxygen diffusion stops when the oxide layer attains a saturation value of ~ 20 monolayers, which is equivalent to ~ 6 nm of oxide.³³ The present observation of continuously increasing FWHM of the oxygen peak with ion fluence is in contrast to the saturation behavior in solid state diffusion. Thus, the present experiment supports the existence of transient thermal spike leading to melt phase, which results in the enhanced oxygen diffusion.

We report the adsorption and subsequent diffusion of oxygen during swift heavy ion irradiation of Fe/Si, the cause of which is related to a transient temperature spike generated by extremely large electronic energy deposition. It results in enhanced diffusion of oxygen during the transient melt phase of Fe. The present work is evidence of the existence of a temperature spike along the ion track in Fe, creating a molten phase for a short duration, during which diffusion of oxygen is believed to have occurred. The present work opens up an area of investigation of ion beam induced absorption, where

the questions such as threshold for such behavior, dependence of absorption on the quantitative value of electronic excitation, similar behavior in other materials with good oxygen affinity, etc., have to be addressed. Present newly observed phenomenon of ion-induced absorption of oxygen has given insight into the ion material interaction.

ACKNOWLEDGMENTS

We (D.K.A. and W.A.) gratefully acknowledge the financial support from the Department of Science and Technology, New Delhi and the Internationales Büro des BMBF, Bonn (under the project DLR code INI-324).

-
- ¹S. Klaumünzer, M.D. Hou, and G. Schumacher, *Phys. Rev. Lett.* **57**, 850 (1986).
- ²A. Audouard, E. Balanzat, S. Bouffard, J.C. Jousset, A. Chamberod, A. Dunlop, D. Lesueur, G. Fuchs, R. Spohr, J. Vetter, and L. Thomé, *Phys. Rev. Lett.* **65**, 875 (1990).
- ³H. Dammak, A. Dunlop, D. Lesueur, A. Brunelle, S. Della-Negra, and Y. Le Beyec, *Phys. Rev. Lett.* **74**, 1135 (1995).
- ⁴R.C. Budhani, M. Suenaga, and S.H. Liou, *Phys. Rev. Lett.* **69**, 3816 (1992).
- ⁵C. Dufour, F. Beuneu, E. Paumier, and M. Toulemonde, *Europhys. Lett.* **45**, 585 (1999).
- ⁶J. L'Ecuyer, C. Brassard, C. Cardinal, and B. Terrault, *J. Appl. Phys.* **47**, 381 (1976).
- ⁷W. Assmann, H. Huber, Th. Reichelt, J.A. Davies, R. Siegele, G. Dollinger, and J.S. Forster, *Nucl. Instrum. Methods Phys. Res. B* **118**, 242 (1996).
- ⁸D.K. Avasthi, W. Assmann, H. Nolte, H.D. Mieskes, and H. Huber, *Nucl. Instrum. Methods Phys. Res. B* **142**, 117 (1998).
- ⁹R.E. Johnson and B.U.R. Sundqvist, *Phys. Today* **45** (3), 28 (1992).
- ¹⁰S. Della-Negra, Y. Le Beyec, B. Monart, K. Standing, and K. Wien, *Phys. Rev. Lett.* **58**, 17 (1987).
- ¹¹M. Toulemonde, W. Assmann, C. Trautmann, and F. Grüner, *Phys. Rev. Lett.* **88**, 057602 (2002).
- ¹²F. Pawlak, C. Dufour, A. Laurent, E. Paumier, and J. Perrire, *Nucl. Instrum. Methods Phys. Res. B* **151**, 140 (1999).
- ¹³H.D. Mieskes, W. Assmann, M. Brodale, M. Dobler, H. Glückler, P. Hartung, and P. Stenzel, *Nucl. Instrum. Methods Phys. Res. B* **146**, 162 (1998).
- ¹⁴H.S. Nagaraja, F. Ohnesorge, D.K. Avasthi, R. Neumann, and P. Mohan Rao, *Appl. Phys. A: Mater. Sci. Process.* **71**, 337 (2000).
- ¹⁵I.A. Baranov, A. Novikov, V. Obnorskii, and C.T. Reimann, *Nucl. Instrum. Methods Phys. Res. B* **146**, 154 (1998).
- ¹⁶S. Ghosh, A. Tripathi, T. Som, S.K. Srivastava, V. Ganesan, A. Gupta, and D.K. Avasthi, *Radiat. Eff. Defects Solids* **154**, 151 (2001).
- ¹⁷S. Bouneau, M. Fallavier, and J.C. Poizat (unpublished).
- ¹⁸R.M. Papaléo, P. Demirev, J. Eriksson, P. Håkansson, and B.U.R. Sundqvist, *Phys. Rev. B* **54**, 3173 (1996); and R.M. Papaléo, *Nucl. Instrum. Methods Phys. Res. B* **131**, 121 (1997).
- ¹⁹A. Gupta and D.K. Avasthi, *Phys. Rev. B* **64**, 155407 (2001).
- ²⁰Z.G. Wang, C. Dufour, E. Paumier, and M. Toulemonde, *J. Phys.: Condens. Matter* **6**, 6773 (1994).
- ²¹Z.G. Wang, C. Dufour, E. Paumier, and M. Toulemonde, *J. Phys.: Condens. Matter* **7**, 2525 (1995).
- ²²C. Dufour, Z.G. Wang, E. Paumier, and M. Toulemonde, *Bull. Mater. Sci.* **22**, 671 (1999).
- ²³D.K. Avasthi, W. Assmann, H. Nolte, H.D. Mieskes, S. Ghosh, and N.C. Mishra, *Nucl. Instrum. Methods Phys. Res. B* **166-167**, 345 (2000).
- ²⁴W. Bolse and B. Schattat, *Nucl. Instrum. Methods Phys. Res. B* **190**, 173 (2002).
- ²⁵A. Audouard, E. Balanzat, G. Fuchs, J.C. Jousset, D. Lesueur, and L. Thome, *Europhys. Lett.* **3**, 327 (1987); **5**, 241 (1988).
- ²⁶H.J. von Bardeleben, D. Stiévenard, D. Deresmes, A. Huber, and J.C. Bourgoin, *Phys. Rev. B* **34**, 7192 (1986).
- ²⁷A. Iwase, S. Sasaki, T. Iwata, and T. Nihira, *Phys. Rev. Lett.* **58**, 2450 (1987).
- ²⁸J.P. Biersack, *Nucl. Instrum. Methods Phys. Res. B* **27**, 21 (1987).
- ²⁹G.H. Olivera, C. Caraby, P. Jardin, A. Cassimi, L. Adoui, and B. Gervais, *Phys. Med. Biol.* **43**, 2347 (1998).
- ³⁰J.H. Swisher and E.T. Turkdogan, *Trans. Metall. Soc. AIME* **239**, 426 (1967).
- ³¹R. Barlow and P.J. Grundy, *J. Mater. Sci.* **4**, 797 (1969).
- ³²J. Takada, S. Yamamoto, and M. Adachi, *Z. Metallkd.* **77**, 6 (1986).
- ³³M. Martin, W. Mader, and E. Fromm, *Thin Solid Films* **250**, 61 (1994).